

**MODELLING BIOLOGICAL MACROMOLECULES IN SOLUTION:
THE GENERAL TRI-AXIAL ELLIPSOID**

Stephen Ernest Harding, M.A. (Oxon), M.Sc.

PhD Dissertation

University of Leicester

1980

CHAPTER 3

Numerical Inversion Procedures:

The Problem of the Line Solution

BIBLIOGRAPHY.

Alexander, A.E. and Johnson, P. (1949)

'Colloid Science', Volume 2, Oxford University Press

Alpert, S.S. and Banks, G. (1976)

Biophysical Chem. 4, 287

Baghurst, P.A., Nichol, L.W., Ogston, A.G., Winzor, D.J. (1975)

Biochem. J. 147, 575

Ballinger, K.W.A. and Jennings, B.R. (1979)

Nature 282, 699

Batchelor, G.K. (1967)

'An Introduction to Fluid Mechanics', Cambridge University Press

Batchelor, G.K. (1970)

J. Fluid Mech. 41, 545

Batchelor, G.K. and Green, J.T. (1972)

J. Fluid Mech. 56, 375

Beeman, W.W., Koesberg, P., Anderegg, J.W. and Webb, M.B. (1957)

in 'Handbuck der Physik', (Flugge, S. ed.), 32, 321, Springer-Verlagg
(Berlin)

Benoit, H. (1951)

Ann. Physik. 6, 561

Berne, P.J. and Pecora, R. (1974)

Ann. Rev. Phys. Chem. 25, 233

Blake, C.C.F. (1975)

Essays in Biochem. II, 37

Blake, C.C.F., Geisow, M.J. and Oatley, S.J. (1978)

J. Mol. Biol. 121, 339

Blake, C.C.F., Koenig, D.F., Mair, G.A., North, A.C.T., Phillips, D.C.
and Sarma, V.R. (1965)

Nature 206, 757

Bloomfield, V.A., Dalton, W.O. and Van Holde, K.E. (1967)

Biopolymers 5, 135

Bresler and Talmud (1944)

CR Acad. Sci. URSS, 43, 310

Brinkman, H.C., Hermans, J.J., Oosterhoff, L.J., Overbeek, J. Th. G.,
Polder, D., Staverman, A.J. and Wiebenga, E.H. (1949)

Proc. Int. Rheol. Congress (Schveningen) II, 77

Brenner, H. (1970)

J. Coll. Int. Sci. 32, 141

Brenner, H. (1972a)

Chem. Eng. Sci. 27, 1069

Brenner, H. (1972b)

Progr. Heat and Mass Transfer 5, 93

Cantor, C.R. and Tao, T. (1971)

Proc. Nucl. Acid Res. 2, 31

Cerf, R. and Scheraga, H.A. (1952)

Chem. Revs. 51, 185

Chapman, P.F. (1913)

Phil. Mag. 25, 475

Cheng, P.Y. and Schachman, H.K. (1955)

J. Polymer Sci. 16, 19

Chu, B. (1974)

'Laser Light Scattering', Academic, New York

Chwang, A.T. (1975)

J. Fluid Mech. 72, 17

Clenshaw, C.W. and Curtis, A.R. (1960)

Num. Math. 2, 197

Creeth, J.M. and Knight, C.G. (1965)

Biochim. Biophys. Acta 102, 549

Cummings, H.Z. and Pike, E.R. (1973)

(eds.) 'Photon Correlation and Light Beating Spectroscopy', Plenum,
New York

Dickerson, R.E. and Geiss, I. (1969)

'The Structure and Action of Proteins', Benjamin, California

Dougherty, J. and Kreiger, I.M. (1972)

in Kreiger, Adv. Colloid Sci. 3, 111

Edsall, J.T. (1953)

in 'The Proteins' (Neurath, H. and Bailey, K. eds) 1B, Chapter 7,
Academic, New York

Edwardes, D. (1892)

Quart. J. Math. 26, 70

Einstein, A. (1905)

Ann. Physik 17, 549

Einstein, A. (1906)

Ann. Physik 34, 591

Einstein, A. (1911)

Ann Physik 34, 591

Emes, C.H. (1977)

Ph. D. thesis, University of Leicester

Emes, C.H. and Rowe, A.J. (1978a)

Biochim. Biophys. Acta 537, 110

Emes, C.H. and Rowe, A.J. (1978b)

Biochim. Biophys. Acta 537, 125

Farrant, J.L. (1954)

Biochim. Biophys. Acta 13, 569

Feldman, R.J. (1976)

'Atlas of Macromolecular Structure on Microfiche', Traco Jitco Int.,
Rockville, Md. USA

Gans, R. (1928)

Ann. Physik 86, 628

García Bernal, J.M. and García de la Torre, J. (1980)

Biopolymers 19, 628

García de la Torre, J. and Bloomfield, V.A. (1977a)

Biopolymers 16, 1747

García de la Torre, J. and Bloomfield, V.A. (1977b)

Biopolymers 16, 1765

Garcia de la Torre, J. and Bloomfield, V.A. (1977c)

Biopolymers 16, 1779

Garcia de la Torre, J. and Bloomfield, V.A. (1978)

Biopolymers 17, 1605

Gardner, D.G., Gardner, J.C., Laush, G. and Meinke, W.W. (1959)

J. Chem. Phys. 31, 978

Giesekeus, H. (1962)

Rheol. Acta 2, 50

Gill, P.E. and Murray, W. (1976)

Nat. Phys. Lab. report NAC 72

Gold, O. (1937)

Ph. D. thesis, University of Vienna

Goodwin, J.W. (1975)

Colloid Science 2 (Chemical Society), 246

Guoy, L.G. (1910)

J. Phys. Chem. 9, 457

Hall, C.E. and Slayter, H.S. (1959)

J. Biophys. Cytol. 5, 11

Harding, S.E. (1980a)

Biochem. J. 189 (in press)

Harding, S.E. (1980b)

mss. submitted to J. Phys. Chem.

Harrison, P.M. (1959)

J. Mol. Biol. 1, 69

Herzog, R.O., Illig, R. and Kudar, H. (1934)

Z. Phys. Chem. A167, 329

Holtzer, A. and Lowey, S. (1956)

J. Am. Chem. Soc. 78, 5954

Jablonski, A. (1961)

Naturforsch 169, 1

Jeffrey, G.B. (1922)

Proc. Roy. Soc. (London) A102, 476

Johnson, P. and Mihalyi, E. (1965)

Biochim. Biophys. Acta 102, 476

Jost, J.W. and O'Konski, C.T. (1978)

in 'Molecular Electro Optics' (O'Konski, C.T. ed.) Volume 2, 529

Kartha, G., Bello, J. and Harker, D. (1967)

Nature 213, 862

Kendrew, J.C., Bodo, G., Dintzis, H.M., Parrish, R.G., Wycoff, H.
and Phillips, D.C. (1958)

Nature 181, 665

Kim, S.H. (1974)

in 'Biochemistry' (Stryer, L.) 653, Freeman, San Francisco

Kirkwood, J.G. (1967)

'Macromolecules' (Aueur, P.L. ed.), Gordon and Breach

Koenig, S.H. (1975)

Biopolymers 14, 2421

Kratky, O., Leopold, H. and Stabinger, H. (1969)

Z. Angew. Phys. 27, 273

Kratky, O., Leopold, H. and Stabinger, H. (1969)

in 'Methods in Enzymology' (Hirs, C.H.W. and Timasheff, S.N. eds.),
27, 98, Academic, London

Krause, S. and O'Konski, C.T. (1959)

J. Am. Chem. Soc. 81, 5082

Kuff, E.J. and Dalton, A.L. (1957)

J. Ultrastructure Res. 1, 62

Kuhn, W. and Kuhn, H. (1945)

Helvetica Chimica Acta 38, 97

Kynch, G.J. (1956)

Proc. Roy. Soc. (London) A237, 90

Labaw, L.W. and Wycoff, R.W.G. (1957)

Biochim. Biophys. Acta 25, 263

Lauffer, M.A. (1942)

Chem. Rev. 31, 561

Laurent, T.C. and Killander, J. (1964)

J. Chromatog. 14, 317

Lipscomb, W.N. (1971)

Proc. Robert A. Welch Found. Conf. Chem. Res. 15, 134

Lloyd, P.H. (1974)

'Optical Methods in Ultracentrifugation, Electrophoresis and Diffusion',

Clarendon Press, Oxford

Lucas, C.W. and Terrill, C.W. (1970)

Collected Algorithms from CACM, No. 404

Manley, R. and Mason, S. G. (1954)

Canad. J. Chem. 32, 763

Martin, R.B. (1964)

'Introduction to Biophysical Chemistry' Chap. 11, McGraw-Hill, New York

McCammon, J.A., Deutch, J.M. and Bloomfield, V.A. (1975)

Biopolymers 14, 2479

Mehl, J.W., Oncley, J.L. and Simha, R. (1940)

Science 92, 132

Mendelson, R. and Hartt, J. (1980)

EMBO Workshop on Muscle Contraction, Alpbach Conf. Austria

Mihalyi, E. and Godfrey, J. (1963)

Biochim. Biophys. Acta 67, 90

Memming, R. (1961)

Z. Physik. Chem. (Frankfurt) 28, 169

Mooney, M. (1951)

J. Coll. Sci. 6, 162

Mooney, M. (1957)

J. Coll. Sci. 12, 575

Munro, I., Pecht, I. and Stryer, L. (1979)

Proc. Nat. Acad. Sci. (USA) 76, 56

Nichol, L.W., Jeffrey, P.D., Turner, D.R. and Winzor, D.J. (1977)

J. Phys. Chem. 81, 776

Nisihara, T. and Doty, P. (1958)

Proc. Nat. Acad. Sci. (USA) 44, 411

Oberbeck, A. (1876)

J. reine. angew. Math. 81, 62

O'Connor, D.V., Ware, W.R. and Andre, J.C. (1979)

J. Phys. Chem. 83, 1333

Offer, G., Moos, C. and Starr, R. (1973)

J. Mol. Biol. 74, 653

O'Hara and Smith (1968)

Comp. Journal 11, 213

O'Konski, C.T. and Haltner, A.J. (1956)

J. Am. Chem. Soc. 78, 3604

Oliver, J. (1972)

Comp. Journal 15, 141

Oncley, J.L. (1940)

J. Phys. Chem. 44, 1103

Oncley, J.L. (1941)

Ann. New York Acad. Sci. 41, 121

Paradine, C.G. and Rivett, B.H.P. (1960)

'Statistical Methods for Technologists', English Universities Press,
London

Pearce, T.C., Rowe, A.J. and Turnock, G. (1975)

J. Mol. Biol. 97, 193

Perrin, F. (1934)

J. Phys. Radium 5, 497

Perrin, F. (1936)

J. Phys. Radium 7, 1

Perutz, M.F., Rossmann, M.G., Cullis, A.F., Muirhead, H., Will, G. and

North, A.C.T. (1960)

Nature 185, 416

Powell, D.R. and MacDonald, J.R. (1972)

Comp. Journal 15, 148

Pytkowickz, R.M. and O'Konski, C.T. (1959)

J. Am. Chem. Soc. 81, 5082

Rallison, J.M. (1978)

J. Fluid Mech. 84, 237

Riddiford, C.L. and Jennings, B.R. (1967)

Biopolymers 5, 757

Ridgeway, D. (1966)

J. Am. Chem. Soc. 88, 1104

Ridgeway, D. (1968)

J. Am. Chem. Soc. 90, 18

Rowe, A.J. (1977)

Biopolymers 16, 2595

Rowe, A.J. (1978)

Techniques in Protein and Enzyme Biochem. B105a, 1

Saito, N. (1951)

J. Phys. Soc. (Japan) 6, 297

Scheraga, H.A. (1955)

J. Chem. Phys. 23, 1526

Scheraga, H.A. (1961)

'Protein Structure', Academic, New York

Scheraga, H.A. and Mandelkern, L. (1953)

J. Am. Chem. Soc. 79, 179

Simha, R. (1940)

J. Phys. Chem. 44, 25

Simha, R. (1952)

J. Appl. Phys. 23, 1020

Shaw, D.J. (1970)

'Introduction to Colloid and Surface Chemistry' (2nd edn.), Butterworths

Small, E.W. and Isenberg, I. (1977)

Biopolymers 16, 1907

Sorenson, N.A. (1930)

CR Lab. Carlsberg 18, No. 5

Squire, P.G. (1970)

Biochim. Biophys. Acta 221, 425

Squire, P.G. (1978)

in 'Molecular Electro Optics' (O'Konski, C.T. ed.) Volume 2, 565

Squire, P.G., Moser, L. and O'Konski, C.T. (1968)

Biochemistry 7, 4261

Stacey, K.A. (1956)

'Light Scattering in Physical Chemistry', Butterworths, London

Stokes, Sir G. (1851)

Trans. Cambridge Phil. Soc. 9, 8

Stokes, Sir G. (1880)

'Mathematical and Physical Papers', Cambridge University Press

Svedberg, T. and Pedersen, K.O. (1940)

'The Ultracentrifuge', Oxford University Press

Tanford, C. (1955)

J. Phys. Chem. 59, 798

Tanford, C. (1961)

'Physical Chemistry of Macromolecules', Wiley, New York

Theorell, H. (1934)

Biochem. Z. 268, 46

Vand, V. (1948)

J. Phys. Coll. Chem. 52, 277

Van de Hulst, H.C. (1957)

'Light Scattering by Small Particles', Wiley, New York

Van Holde, K.E. (1971)

'Physical Biochemistry', Prentice Hall, New Jersey

Wahl, P. (1966)

Compt. Rend. Acad. Sci. (Paris) 263D 1525

Wales, M. and Van Holde, K.E. (1954)

J. Polymer Sci. 14, 81

Wilde, D.J. (1964)

'Optimum Seeking Methods', Prentice Hall, New Jersey

Williams, R.C., Ham, W.T. and Wright, A.K. (1976)

Anal. Biochem. 73, 52

Wilson, R.W. and Bloomfield, V.A. (1979a)

Biopolymers 18, 1205

Wilson, R.W. and Bloomfield, V.A. (1979b)

Biopolymers 18, 1543

Yang, J.T. (1961)

Adv. Protein Chem. 16, 323

Zimm, B.H. (1948)

J. Chem. Phys. 16, 1093

Zimm, B.H. (1956)

J. Chem. Phys. 24, 269

3.1 Solution of the Elliptic Integrals

In order to determine the viscosity increment v that corresponds to a particular value of the axial ratios a/b , b/c , the elliptic integrals α_0 etc. (Appendix I) must be solved. Analytic solutions are not possible but the integrals can be solved numerically with the aid of a high speed computer. The subroutine used for this was the United Kingdom NAG Mk. 6 routine D01AGF which evaluates a definite integral of the form

$$I = \int_A^B f(t) dt$$

where $A=0$, using an interval subdivision strategy developed by Oliver (1972) and based on Clenshaw-Curtis quadrature (1960). Since infinity cannot be used as the upper limit, a finite value of B must be specified. However, a satisfactory value for B can be determined by using successively higher values until the value of the integral converges to a limiting value; in this case a value for B of 10^6 was sufficient. Higher values are also suitable although evaluation of the integral takes longer. The number of interval subdivisions is also specifiable by the user; the maximum number of 50 was used. The routine also estimates the error on the integrals (O'Hara & Smith, 1968). If this error is greater than the maximum allowable error specifiable by the user the routine will stop and print an error message. The maximum allowed absolute error specified was 1.0×10^{-8} ($\approx .001\%$). The subroutine for evaluating the elliptic integrals can easily be incorporated into a program for evaluating v for a given value of $(a/b, b/c)$. This is given in Appendix V as Program 1.

3.2. Application to the Crystallographic Dimensions of Myoglobin;

Numerical Inversion

The result can be applied to crystallographic data available for myoglobin. Kendrew et al (1958) gave the dimensions of sperm whale myoglobin to be $43 \times 35 \times 23 \text{ \AA}$ (Table 3). This corresponds to a general tri-axial ellipsoid of semi-axes $a = 21.5$, $b = 17.5$ and $c = 11.5 \text{ \AA}$, and axial ratios $a/b = 1.23$, $b/c = 1.52$. Using Program 1 (Appendix V) this corresponds to a viscosity increment of 2.729. The predicted intrinsic viscosity can then be found from equation (8):

$$[\eta] = v \bar{v}_s \equiv v \bar{v} \left(\frac{\bar{v}_s}{\bar{v}} \right) \quad (92)$$

where (\bar{v}_s/\bar{v}) is the swelling ratio (section 1.7.1). By fitting data of reduced specific viscosity against concentration (Table 8, Figure 27) I have determined the intrinsic viscosity of myoglobin to be $(3.25 \pm .05)$ ml/gm, using a weighted least squares analysis (straight line fit). The concentrations were determined using a high precision auto density meter (Kratky et al, 1969, 1973) together with a \bar{v} for myoglobin of .741 ml/gm (Theorell, 1934):

$$c_i = \frac{\rho_i - \rho_o}{1 - \bar{v}\rho_o} \quad (93)$$

where ρ_o is the solvent density and ρ_i the solute densities. Use of the auto density meter, which is based on the time taken to perform a preset number of oscillations of a U-tube filled with the sample has the added advantage that, besides being very accurate, only small amounts of fluid are required (~ 1 ml). The experimental arrangement used for the viscosity and densimetric work is illustrated in Figure 28. The

platinum resistance thermometer shown was used to monitor the sample temperatures to accuracies of .005 degrees and was calibrated by myself. In order that the crystallographic dimensions gives this same value for $[\eta]$, from equation (92), a swelling ratio (\bar{v}_s/\bar{v}) of 1.6 is required; alternatively myoglobin is more asymmetric in solution.

In order to determine the actual dimensions of the equivalent tri-axial ellipsoid for myoglobin in solution (or any other macromolecule) from the experimental value for $[\eta]$, the situation is more complicated however. Although equation (88) defines a unique value of v for a given value of $(a/b, b/c)$, an analytic inversion of (88) to produce an explicit expression for $(a/b, b/c)$ in terms of v is not available. The inversion must therefore be done numerically by tabulating, or better plotting v as a function of $(a/b, b/c)$. The same subroutine mentioned in section 3.1. *for evaluating the elliptic integrals may* be incorporated. A perusal of Table 7 (produced from Program 2) reveals however that a given value of v does not correspond to a unique value of $(a/b, b/c)$ but to a 'line solution' of possible values of $(a/b, b/c)$. This is clearly illustrated in the contour plot (Figure 29) produced from Program 3 using GHOST graphical facilities where v is incremented from 2.5 to 7.0 in steps of 0.5. In order to determine a unique solution for $(a/b, b/c)$ and hence the axial dimensions of a macromolecule in solution other hydrodynamic information must be used; we must therefore consider the translational and rotational frictional properties (section 1.2).

3.3. Other Tri-axial Line Solutions

3.3.1. The Translational Frictional Ratio; the β and R Functions

It was previously stated in section 1.4. that although Perrin (1936) had provided an explicit formula for the translational frictional ratio of a general tri-axial ellipsoid in terms of the axial ratios (a/b , b/c), the elliptic integral in equation (12) could only be solved analytically for the special case of ellipsoids of revolution (i.e. two equal axes). However, since the elliptical integral is similar to those for the tri-axial viscosity increment, it too can now be solved numerically using for example the subroutine discussed in section 3.1. A higher value for the upper limit, B was required: 5×10^7 . A table of values of the Perrin function f/f_0 ($\equiv P$) for values of a/b and b/c was thus obtained (Table 9). Again, a perusal of the table reveals that a given value of P has a line solution of possible values of (a/b , b/c). However, in principle at least, by combining the line solution for P of a given macromolecule with the line solution for ν , a unique solution for (a/b , b/c) can in principle be found from their intersection. This can be illustrated by assuming a particle of (a/b , b/c) = (1.5, 1.5), calculating the corresponding values for ν and P using Program 1, and then plotting the line solutions using Program 4. Unfortunately Figure 30 reveals that the intersection for accuracies in ν and P to four significant figures is very shallow, and allowing for $\pm 1\%$ experimental error in each there is no intersection at all in the 'globular protein' range of the Figure. There is also the additional problem that in order to determine experimentally both ν and P , knowledge is required of the swollen volume in solution.

However, now that v and P are available for tri-axial ellipsoids, then so should the β and R functions which do not require a knowledge of the swollen volume (equations 45 & 64). I have thus produced tables of these also (Tables 10 & 11); all four tri-axial functions so far mentioned viz v , P , β and R are plotted in Figure 31 allowing for $\pm 1\%$ experimental error in each. There is still no reasonable intersection; the β function is, as expected, seen to be of little practical use as it is very sensitive to experimental error (the $\beta - 1\%$ line is completely off the map area). Of the 4 functions however, the R function is the most useful since it is relatively insensitive to experimental error and the experimental determination does not require a knowledge of the swollen volume (section 1.7.1.). In order to find a unique solution for $(a/b, b/c)$ therefore, this should ideally be combined with a rotational frictional or relaxation tri-axial shape function which should satisfy the following criteria:

- (i) provides a suitable intersection with R
- (ii) is relatively insensitive to experimental error but sensitive to axial ratio
- (iii) is experimentally measurable to a high precision with currently available apparatus and data analytic techniques and
- (iv) does not require a knowledge of the swollen volume for its experimental determination.

3.3.2. The Rotational Frictional, Diffusion and Relaxation Line Solutions

For a tri-axial ellipsoid there will be three rotational frictional ratios ζ_i/ζ_0 ($i=a,b,c$) corresponding to rotation about each of the three axes and hence three rotational diffusion ratios θ_i/θ_0 . By analogy with the translational case in the previous section, although Perrin (1934) had

given explicit formula for the τ_i/τ_0 in terms of $(a/b, b/c)$, - eqn. (25), the elliptic integrals could only be solved analytically for the case of ellipsoids of revolution. The integrals can now be solved numerically, again utilising the routine described in section 3.1 (Programs 1,2 & 4). There is however no experimental technique for determining the rotational frictional or diffusion coefficients directly; rotational experiments determine rather relaxation time ratios. For example, the dielectric dispersion relaxation time ratios are related to the rotational frictional and diffusion ratios by equations (27). A plot of the rotational relaxation time ratio line solutions corresponding to $(a/b, b/c) = (1.5, 1.5)$ is given together with the R function in Figure 32. Unfortunately, because of the difficulties raised in 1.5.1. resolution of the dielectric dispersion curve into the 3 relaxation times for a homogeneous solution of tri-axial ellipsoid particles is impossible in practice.

Whereas for ellipsoids of revolution there are three fluorescence anisotropy decay times (equation 42), for general tri-axial ellipsoids, there will be five (Cantor & Tao, 1971, Small & Isenberg, 1977) related to the three rotational diffusion coefficients by:

$$\begin{aligned} \tau_1 &= \frac{1}{3(\theta + \theta_1)} & ; & \quad \tau_2 = \frac{1}{3(\theta + \theta_2)} & ; & \quad \tau_3 = \frac{1}{3(\theta + \theta_3)} \\ \tau_4 &= \frac{1}{2(3\theta - \Delta)} & ; & \quad \tau_5 = \frac{1}{2(3\theta + \Delta)} \end{aligned} \quad (94)$$

where $\theta = (\theta_1 + \theta_2 + \theta_3)/3$ is the mean rotational diffusion coefficient, and Δ is defined by

$$\Delta = (\theta_1^2 + \theta_2^2 + \theta_3^2 - \theta_1\theta_2 - \theta_2\theta_3 - \theta_3\theta_1)^{\frac{1}{2}}$$

The fluorescence anisotropy relaxation time ratios τ_j / τ_0 can thus be evaluated (equation 42, where j is now = 1,2,3,4,5); these have been tabulated by Small & Isenberg (1977) and are plotted in Figure 33, for $(a/b, b/c) = (1.5, 1.5)$. Consideration of these functions however, at the moment at least, is purely academic; besides the problems cited in section 1.5.4., the necessary resolution of the decay curve into its four component exponentials (since $\tau_5 \sim \tau_1$) is impossible (Small & Isenberg, 1977). Furthermore, since neither the fluorescence anisotropy decay time ratios nor the dielectric dispersion relaxation time ratios for tri-axial ellipsoids are of apparent use at the moment, the same must be true of their corresponding swelling independent functions, the explicit expressions in terms of axial ratio being obtainable from:

$$\delta_i = \frac{\zeta_0}{\zeta_i} v \quad ; \quad \mu_i = \left(\frac{f_0}{f_i}\right) \left(\frac{\zeta_i}{\zeta_0}\right)^{1/3} \quad (95, 96)$$

$$\gamma_i = \left(\frac{f}{f_0}\right)^3 \frac{\rho_0}{\rho_i} \quad ; \quad \epsilon_i = v \frac{\rho_0}{\rho_i} \quad (97, 98)$$

$$\kappa_j = v \left(\frac{\tau_0}{\tau_j}\right) \quad ; \quad \xi_j = \left(\frac{f}{f_0}\right)^3 \frac{\tau_0}{\tau_j} \quad (99, 100)$$

where $i=a,b,c$ and $j=1,2,3,4,5$. The relations for these functions in terms of experimental parameters have already been given in section 1.7.

Evaluation of the harmonic mean rotational relaxation time ratio in terms of axial ratio for tri-axial ellipsoids we can similarly obtain from

$$\frac{\tau_h}{\tau_o} = \frac{3}{\left(\frac{\rho_o}{\rho_a} + \frac{\rho_o}{\rho_b} + \frac{\rho_o}{\rho_c} \right)} \quad (101)$$

(Programs 1, 2 & 4, Figure 34). The corresponding swelling independent functions Ψ and Λ determined by combining with the translational frictional ratio and the viscosity increment respectively we can now also obtain from

$$\Psi = \left(\frac{\tau_o}{\tau_h} \right)^{1/3} \left(\frac{f}{f_o} \right) \quad (102)$$

$$\Lambda = \left(\frac{\tau_o}{\tau_h} \right) \nu \quad (103)$$

(Programs 1,2 & 4, Figure 34). Unfortunately, these functions are generally very sensitive to experimental error, as Figure 35 illustrates; also the problems in determining the harmonic mean relaxation time raised in 1.5.4. still apply.

3.3.3 Electric Birefringence Decay: the δ_+ and δ_- Functions

In section 1.5.2. we stated that Ridgeway (1966, 1968) has shown that the decay of electric birefringence for a homogeneous suspension of asymmetric macromolecules (e.g. tri-axial ellipsoids) would consist of two exponential terms:

$$\Delta n = \frac{N}{2n_l} \left\{ A_+ e^{-6\theta_+ t} + A_- e^{-6\theta_- t} \right\} \quad (32)$$

where Δn is the birefringence, N the number density of particles in suspension and n_ℓ the refractive index of the suspending medium. A_+ and A_- are complicated functions depending on the initial orientation of the particles and their dielectric and diffusion properties. We may rewrite $NA_\pm / 2n_\ell$ as A'_\pm , the 'pre-exponential factors'. Equation (32) then becomes:

$$\Delta n = A'_+ e^{-6\theta_+ t} + A'_- e^{-6\theta_- t} \quad (104)$$

θ_+ and θ_- are related to the rotational diffusion constants θ_i (and hence the rotational frictional coefficients since $\zeta_i = kT/\theta_i$) by

$$\theta_\pm = \frac{1}{3} \sum \theta_i \pm \left\{ \left(\frac{1}{3} \sum \theta_i \right)^2 - \frac{1}{3} \sum_{i>j} \theta_i \theta_j \right\}^{\frac{1}{2}} \quad (105a)$$

$$= \frac{kT}{3} \left\{ \sum_i \frac{1}{\zeta_i} \pm \left[\sum_i \frac{1}{\zeta_i^2} - \sum_{i>j} \frac{1}{\zeta_i \zeta_j} \right]^{\frac{1}{2}} \right\} \quad (105b)$$

The dimensions of equation (105) are of energy/(volume x viscosity); we therefore 'reduce' it to a function of shape alone:

$$\begin{aligned} \theta_\pm^{\text{red}} &\equiv \left(\frac{\eta_0}{kT} \right) v_e \theta_\pm = \frac{abc}{12} \left\{ \left(\frac{1}{\zeta_a''} + \frac{1}{\zeta_b''} + \frac{1}{\zeta_c''} \right) \right. \\ &\quad \left. \pm \left[\left(\frac{1}{\zeta_a''^2} + \frac{1}{\zeta_b''^2} + \frac{1}{\zeta_c''^2} \right) - \left(\frac{1}{\zeta_a'' \zeta_b''} + \frac{1}{\zeta_b'' \zeta_c''} + \frac{1}{\zeta_c'' \zeta_a''} \right) \right]^{\frac{1}{2}} \right\} \quad (106) \end{aligned}$$

where

$$\zeta_a'' = \frac{b^2 + c^2}{b^2 \beta_0 + c^2 \gamma_0}; \quad \zeta_b'' = \frac{c^2 + a^2}{c^2 \gamma_0 + a^2 \alpha_0}; \quad \zeta_c'' = \frac{a^2 + b^2}{a^2 \alpha_0 + b^2 \beta_0} \quad (107)$$

The elliptic integrals α_0 etc. are those defined by Jeffrey (1922) and are given in Appendix I.

A plot of the θ_+^{red} and θ_-^{red} functions, together with the R function corresponding to the point $(a/b, b/c) = (1.5, 1.5)$ allowing for $\pm 1\%$ experimental error is given in Figure 36. It is seen that the intersections are very reasonable (the θ_+^{red} - R intersection is nearly orthogonal) and the functions are relatively sensitive to axial ratio. However, experimental determination of $\theta_{\pm}^{\text{red}}$ requires of course knowledge of the swollen molecular volume in solution (equation 106). This can be conveniently eliminated however in the standard way by combining (106) either with the viscosity increment (8) or the translational frictional ratio (20b). If for example (106) is combined with the viscosity increment (8), swelling independent δ_{\pm} functions are produced (Tables 12, 13, Figure 37):

$$\delta_{\pm} = 6\theta_{\pm}^{\text{red}} v \equiv \frac{6}{N_A k} \left(\frac{\eta_0 \theta_{\pm}}{T} \right) [\eta] M_r \quad (108)$$

where $[\eta]$ is expressed in ml/gm. Alternatively, $\theta_{\pm}^{\text{red}}$ can be combined with the translational frictional ratio (20b) to give swelling independent γ_{\pm} functions (Programs 1,2,4, Figure 38):

$$\gamma_{\pm} = 6\theta_{\pm}^{\text{red}} \left(\frac{f}{f_0} \right)^3 \equiv \frac{M_r^3 (1 - \bar{v} \rho_0)^3 \theta_{\pm}}{27 N_A k T \pi^2 \eta_0^2 s^3} \quad (109)$$

The δ_{\pm} and γ_{\pm} functions are new. The δ_{\pm} functions are preferred over the γ_{\pm} functions since they require fewer experimental measurements and do not involve squared or cubed terms; hence in principle can be measured more

accurately. It is seen therefore that combination of the R-function with the δ_{\pm} functions as a method for determining a unique solution for the axial ratios (and hence the axial dimensions, if V_g is known from k_{η}/k_s - section 1.7.1) of a macromolecule in solution satisfies the criteria (i), (ii) and (iv) of section 3.3.1. In order for the method to satisfy criterion (iii) however, there still remains the problem of resolving the exponential decay term into its 2 component relaxation times or decay constants (the same is true of course for the $\theta_{\pm}^{\text{red}}$ and γ_{\pm} functions). To date this has not been possible. We now show that with a new 'constrained' least squares algorithm using intersection with the R-curve as the constraint, this is now possible with currently available experimental precision.

Table 8. Values of reduced specific viscosity for various concentrations of sperm whale myoglobin (0.1M NaCl buffer, pH = 7.1)

Concentration, c (mg/ml)	η_{rel}	η_{sp}/c (ml/gm)
90.2	1.450	4.99
66.1	1.298	4.51
53.3	1.224	4.20
50.2	1.215	4.29
40.7	1.163	4.00
34.4	1.138	4.02
30.5	1.116	3.81
29.6	1.115	3.89
23.2	1.084	3.61
15.5	1.055	3.57
9.7	1.034	3.47
8.1	1.028	3.50

Table 9. Values of P as a function of (a/b, b/c) for a general tri-axial ellipsoid (a>b>c)

$\frac{a/b}{b/c}$		Prolate Ellipsoid										
		1.0	1.1	1.2	1.3	1.4	1.5	1.6	1.7	1.8	1.9	2.0
Oblate Ellipsoid	1.0	1.000	1.001	1.003	1.006	1.010	1.014	1.019	1.025	1.030	1.036	1.042
	1.1	1.001	1.002	1.005	1.009	1.014	1.019	1.024	1.030	1.036	1.042	1.049
	1.2	1.003	1.005	1.009	1.013	1.018	1.024	1.030	1.036	1.043	1.049	1.056
	1.3	1.006	1.009	1.013	1.018	1.024	1.030	1.037	1.043	1.050	1.057	1.064
	1.4	1.010	1.014	1.019	1.024	1.030	1.037	1.044	1.051	1.058	1.065	1.073
	1.5	1.015	1.019	1.024	1.031	1.037	1.044	1.051	1.059	1.066	1.074	1.082
	1.6	1.020	1.025	1.031	1.037	1.044	1.052	1.059	1.067	1.075	1.083	1.091
	1.7	1.026	1.031	1.037	1.044	1.052	1.060	1.068	1.076	1.084	1.092	1.101
	1.8	1.031	1.037	1.044	1.052	1.059	1.068	1.076	1.085	1.093	1.102	1.111
	1.9	1.038	1.044	1.051	1.059	1.067	1.076	1.085	1.093	1.102	1.111	1.120
	2.0	1.044	1.051	1.059	1.067	1.075	1.084	1.093	1.102	1.112	1.121	1.130

Table 10. Values of $\beta \times 10^{-6}$ as a function of (a/b, b/c) for a general triaxial ellipsoid (a>b>c)

<div> <div>a/b</div> <div>b/c</div> </div>		Prolate Ellipsoid										
		1.0	1.1	1.2	1.3	1.4	1.5	1.6	1.7	1.8	1.9	2.0
Oblate Ellipsoid	1.0	2.111	2.112	2.112	2.113	2.113	2.114	2.115	2.116	2.117	2.117	2.118
	1.1	2.112	2.112	2.113	2.113	2.114	2.115	2.116	2.117	2.118	2.118	2.119
	1.2	2.112	2.113	2.114	2.114	2.115	2.116	2.117	2.118	2.119	2.120	2.121
	1.3	2.113	2.114	2.115	2.116	2.117	2.118	2.119	2.120	2.121	2.122	2.123
	1.4	2.114	2.115	2.117	2.118	2.119	2.120	2.121	2.123	2.124	2.125	2.126
	1.5	2.116	2.117	2.119	2.120	2.121	2.123	2.124	2.125	2.127	2.128	2.129
	1.6	2.118	2.119	2.121	2.123	2.124	2.126	2.127	2.129	2.130	3.131	2.132
	1.7	2.120	2.122	2.123	2.125	2.127	2.129	2.130	2.132	2.133	2.135	2.136
	1.8	2.122	2.124	2.126	2.128	2.130	2.132	2.134	2.136	2.137	2.139	2.140
	1.9	2.124	2.127	2.129	2.131	2.134	2.136	2.138	2.139	2.141	2.143	2.144
	2.0	2.127	2.130	3.132	2.135	2.137	2.139	2.141	2.143	2.145	2.147	2.149

Table 11. Values of R as a function of (a/b, b/c) for a general tri-axial ellipsoid ($a > b > c$)

$\begin{array}{c} b/c \\ a/b \end{array}$		Prolate Ellipsoid										
		1.0	1.1	1.2	1.3	1.4	1.5	1.6	1.7	1.8	1.9	2.0
Oblate Ellipsoid	1.0	1.600	1.598	1.592	1.583	1.573	1.561	1.548	1.535	1.521	1.507	1.494
	1.1	1.598	1.593	1.585	1.575	1.563	1.549	1.536	1.521	1.507	1.493	1.478
	1.2	1.592	1.585	1.575	1.563	1.549	1.535	1.520	1.505	1.490	1.475	1.460
	1.3	1.582	1.573	1.561	1.548	1.533	1.518	1.502	1.486	1.471	1.455	1.440
	1.4	1.570	1.559	1.546	1.531	1.515	1.499	1.483	1.466	1.450	1.435	1.419
	1.5	1.556	1.543	1.529	1.513	1.496	1.479	1.462	1.445	1.429	1.413	1.397
	1.6	1.540	1.526	1.511	1.494	1.476	1.459	1.441	1.424	1.407	1.391	1.375
	1.7	1.524	1.509	1.491	1.474	1.455	1.437	1.419	1.402	1.385	1.368	1.352
	1.8	1.507	1.490	1.472	1.453	1.434	1.416	1.398	1.380	1.362	1.346	1.330
	1.0	1.489	1.471	1.452	1.433	1.413	1.394	1.376	1.358	1.340	1.324	1.307
	2.0	1.471	1.452	1.432	1.412	1.392	1.373	1.354	1.336	1.318	1.302	1.285

Table 12. Values of δ_+ as a function of (a/b, b/c) for a general tri-axial ellipsoid (a>b>c)

$\frac{a/b}{b/c}$		Prolate Ellipsoid	1.0	1.1	1.2	1.3	1.4	1.5	1.6	1.7	1.8	1.9	2.0
		1.0	1.1	1.2	1.3	1.4	1.5	1.6	1.7	1.8	1.9	2.0	2.0
Oblate Ellipsoid	1.0	2.500	2.541	2.568	2.582	2.588	2.586	2.579	2.568	2.555	2.539	2.522	
	1.1	2.549	2.577	2.596	2.605	2.606	2.601	2.595	2.279	2.564	2.547	2.529	
	1.2	2.599	2.624	2.641	2.648	2.648	2.642	2.632	2.619	2.604	2.587	2.570	
	1.3	2.648	2.675	2.692	2.700	2.700	2.695	2.686	2.674	2.660	2.644	2.627	
	1.4	2.699	2.729	2.748	2.757	2.759	2.756	2.748	2.737	2.724	2.710	2.694	
	1.5	2.752	2.785	2.807	2.818	2.823	2.821	2.815	2.806	2.795	2.781	2.767	
	1.6	2.806	2.844	2.868	2.883	2.890	2.891	2.887	2.880	2.870	2.858	2.845	
	1.7	2.863	2.905	2.933	2.951	2.961	2.965	2.963	2.958	2.949	2.939	2.927	
	1.8	2.922	2.968	3.001	3.023	3.036	3.042	3.042	3.039	3.033	3.024	3.014	
	1.9	2.983	3.035	3.071	3.097	3.113	3.122	3.125	3.124	3.120	3.113	3.104	
	2.0	3.047	3.103	3.145	3.174	3.194	3.206	3.212	3.213	3.210	3.205	3.198	

Table 13. Values of δ as a function of (a/b, b/c) for a general tri-axial ellipsoid (a>b>c)

$\frac{a/b}{b/c}$		Prolate Ellipsoid										
		1.0	1.1	1.2	1.3	1.4	1.5	1.6	1.7	1.8	1.9	2.0
Oblate Ellipsoid	1.0	2.500	2.454	2.413	2.377	2.344	2.314	2.286	2.259	2.235	2.212	2.190
	1.1	2.445	2.410	2.372	2.337	2.305	2.274	2.246	2.220	2.195	2.172	2.151
	1.2	2.387	2.350	2.313	2.277	2.245	2.214	2.185	2.159	2.134	2.111	2.089
	1.3	2.326	2.286	2.248	2.212	2.178	2.147	2.118	2.091	2.066	2.043	2.021
	1.4	2.264	2.222	2.183	2.146	2.112	2.081	2.051	2.024	1.999	1.976	1.954
	1.5	2.203	2.160	2.119	2.082	2.048	2.016	1.987	1.961	1.936	1.913	1.892
	1.6	2.144	2.100	2.059	2.021	1.987	1.956	1.927	1.901	1.877	1.854	1.834
	1.7	2.087	2.042	2.001	1.964	1.930	1.899	1.871	1.845	1.822	1.800	1.780
	1.8	2.033	1.987	1.946	1.910	1.876	1.846	1.819	1.794	1.771	1.750	1.730
	1.9	1.981	1.936	1.895	1.859	1.826	1.797	1.770	1.746	1.724	1.703	1.685
	2.0	1.932	1.887	1.847	1.812	1.780	1.751	1.725	1.702	1.680	1.661	1.643

Figure 27. Plot of reduced specific viscosity versus concentration for sperm whale myoglobin (0.1M NaCl, buffer, pH = 7.1)

The straight line is that due to a weighted least squares fit to $\frac{\eta_{sp}}{c} = [\eta] (1 + k_{\eta} c)$ where $[\eta] = 3.25 \text{ ml/gm}$ and $k_{\eta} = 5.9 \text{ ml/gm}$.

The weight used was $\frac{1}{\text{concentration (mg/ml)}}$ (conc. < 40 mg/ml)

$\frac{1}{40}$ (conc. $\geq 40 \text{ mg/ml}$)

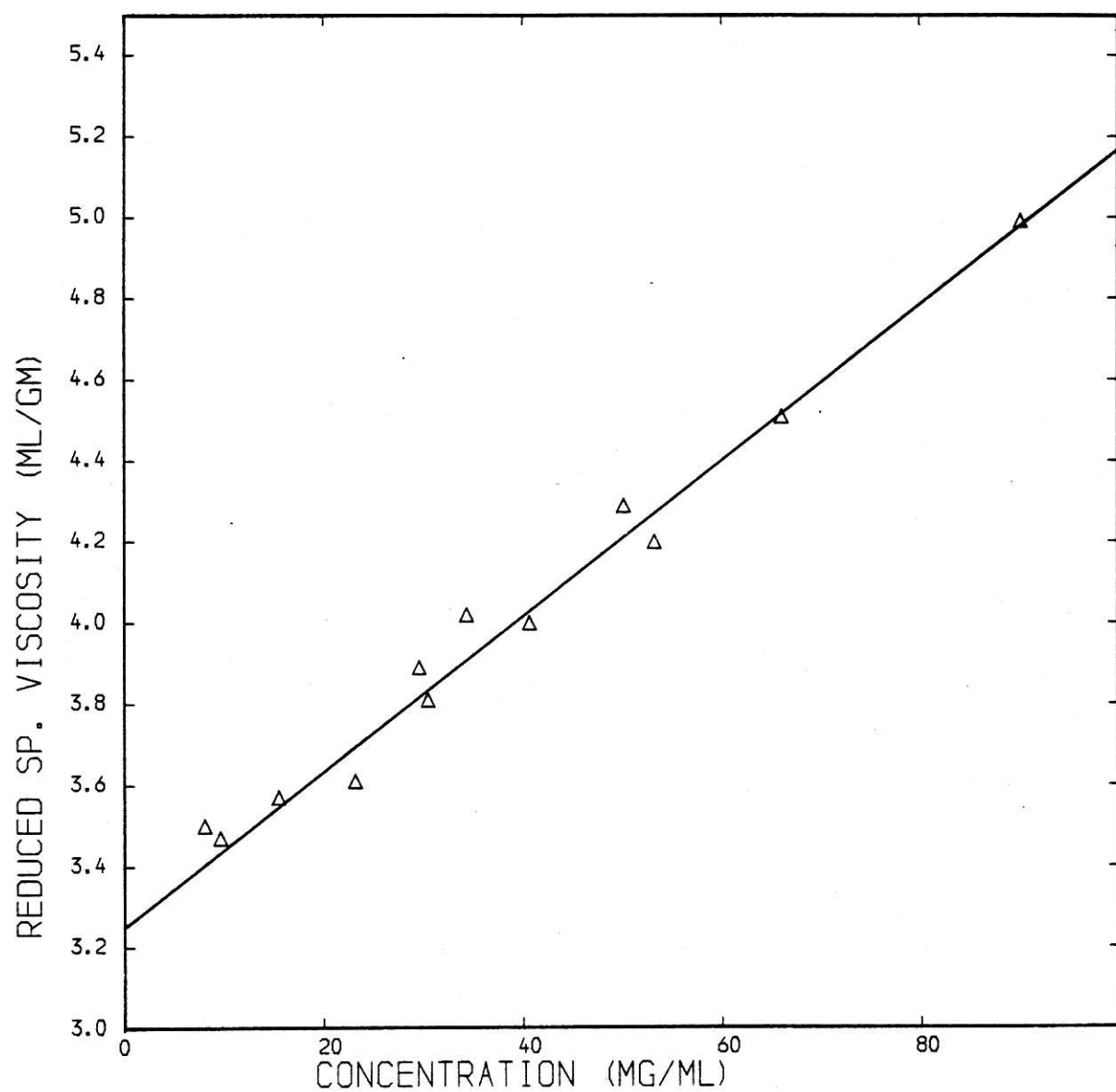
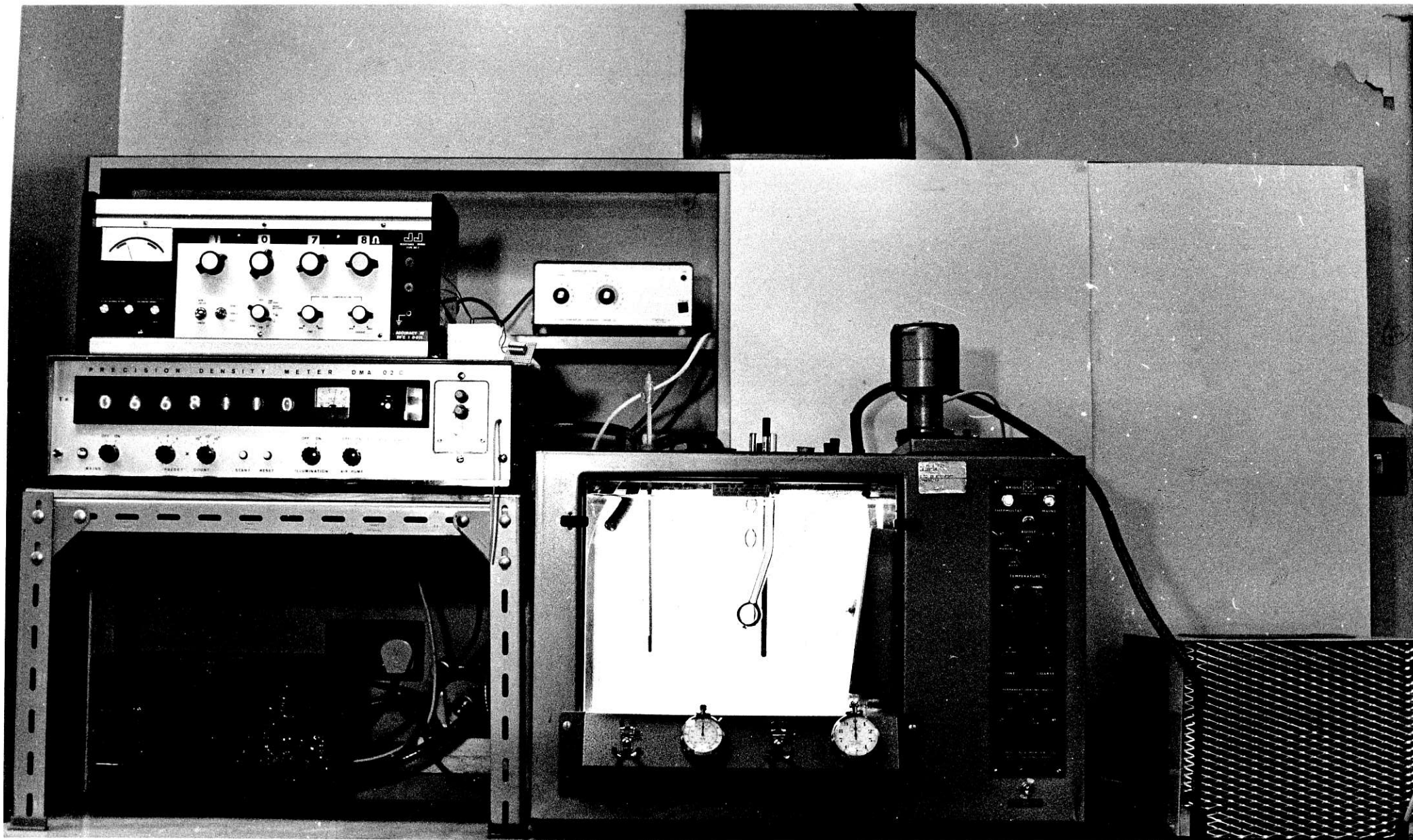


Figure 28. Photograph of the apparatus used for determining solution densities and viscosities. Temperatures were kept constant to within $\pm 0.01^{\circ}$ using a high precision Townson - Mercer constant temperature tank, with a pump attachment to supply the water bath in the precision density meter. These temperatures could be monitored to within $\pm 0.005^{\circ}$ using the platinum resistance thermometer situated directly above the density meter.



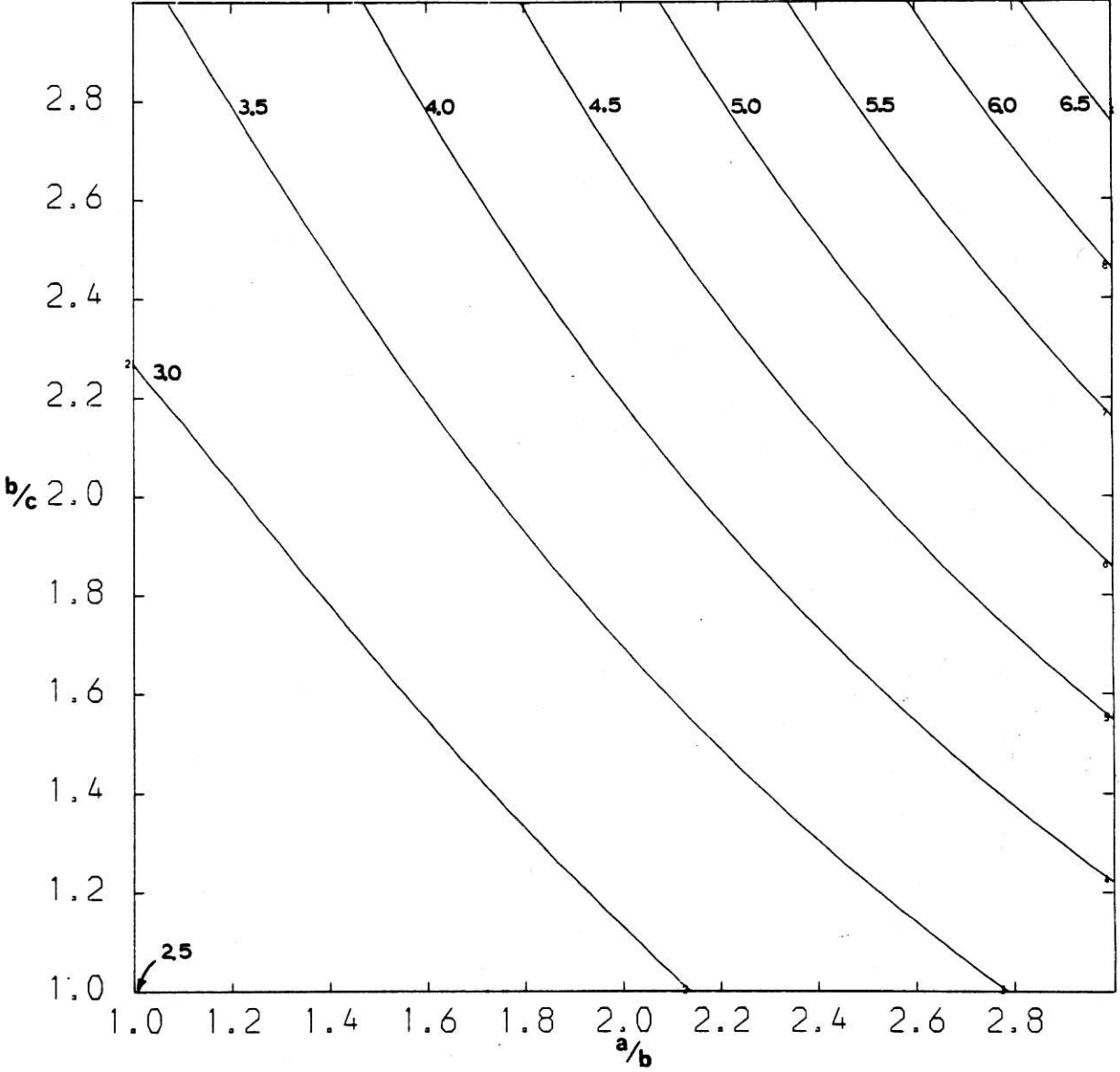


Figure 29. Contour diagram showing curves of constant v as a function of the semi-axial ratios a/b , b/c on the basis of equation (88)

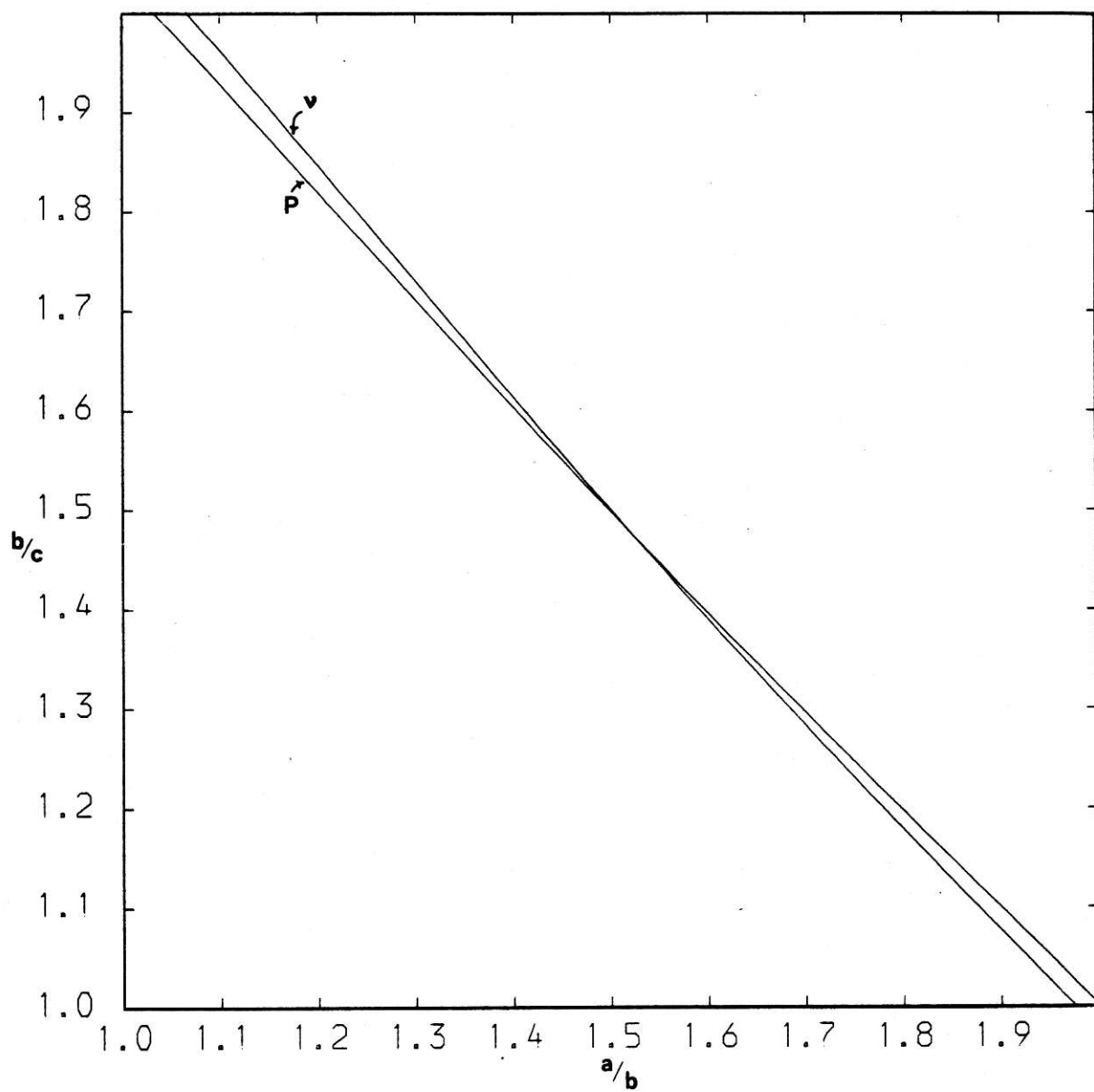


Figure 30. Plots of constant ν and P in the $(a/b, b/c)$ plane corresponding to $a/b = 1.5, b/c = 1.5$

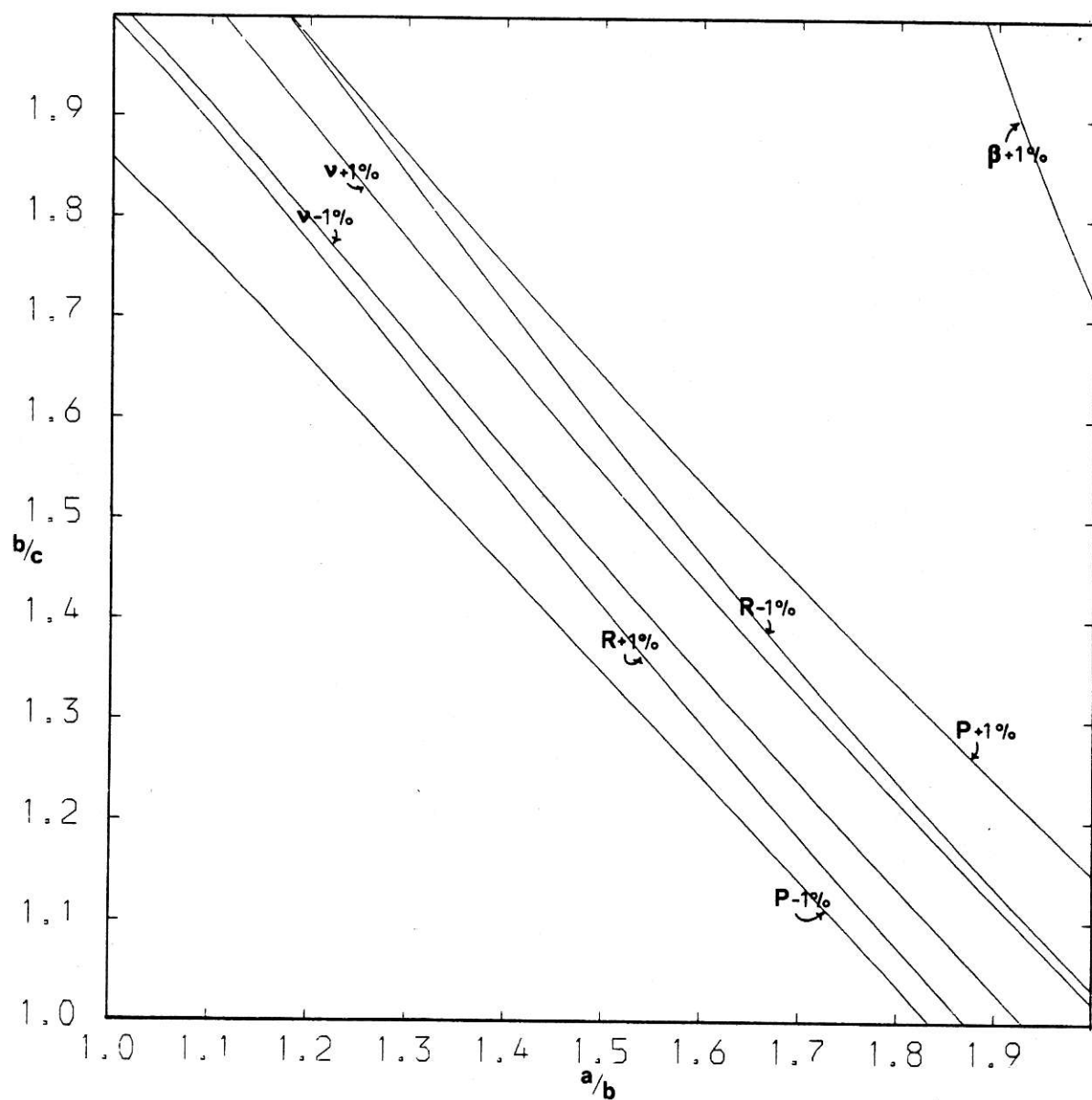


Figure 31. Plots of constant ν , P , β and R , allowing for $\pm 1\%$ error in their measured values, in the a/b , b/c plane corresponding to $a/b = 1.5$, $b/c = 1.5$

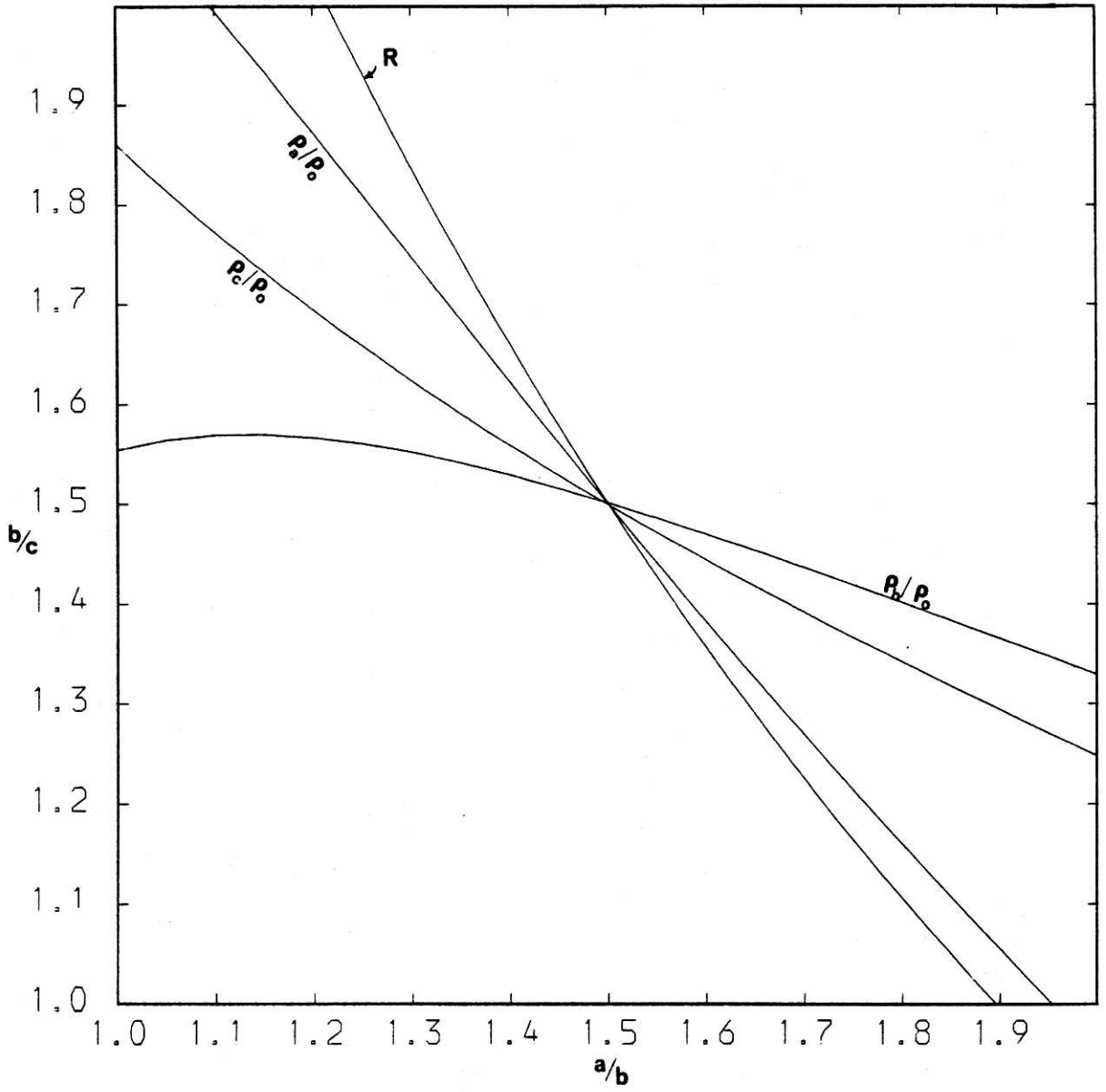


Figure 32. Plots of constant R and the rotational relaxation time ratios in the a/b , b/c plane corresponding to $a/b = 1.5$, $b/c = 1.5$

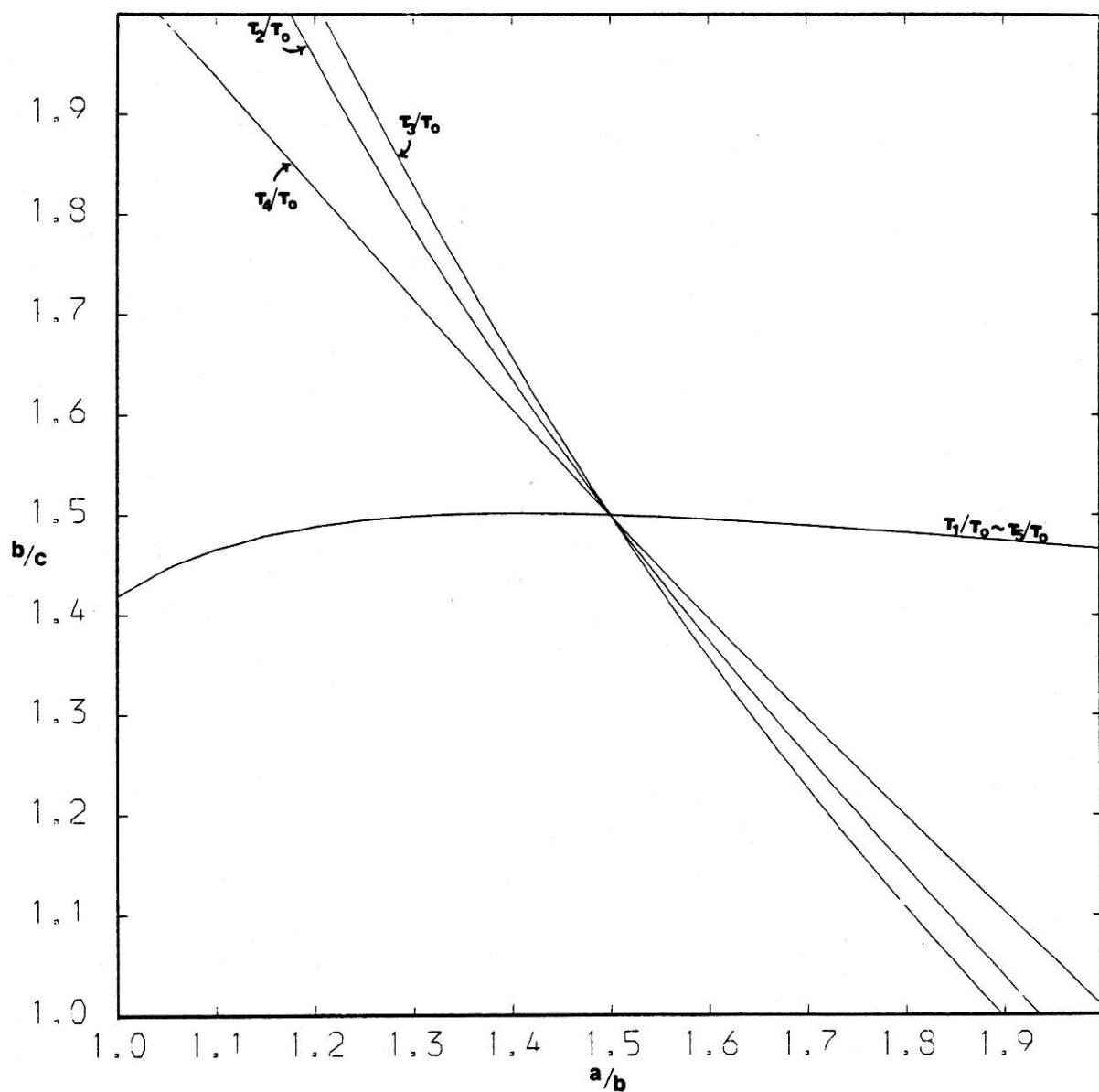


Figure 33. Plots of constant fluorescence anisotropy relaxation time ratios in the a/b , b/c plane corresponding to $a/b = 1.5$, $b/c = 1.5$

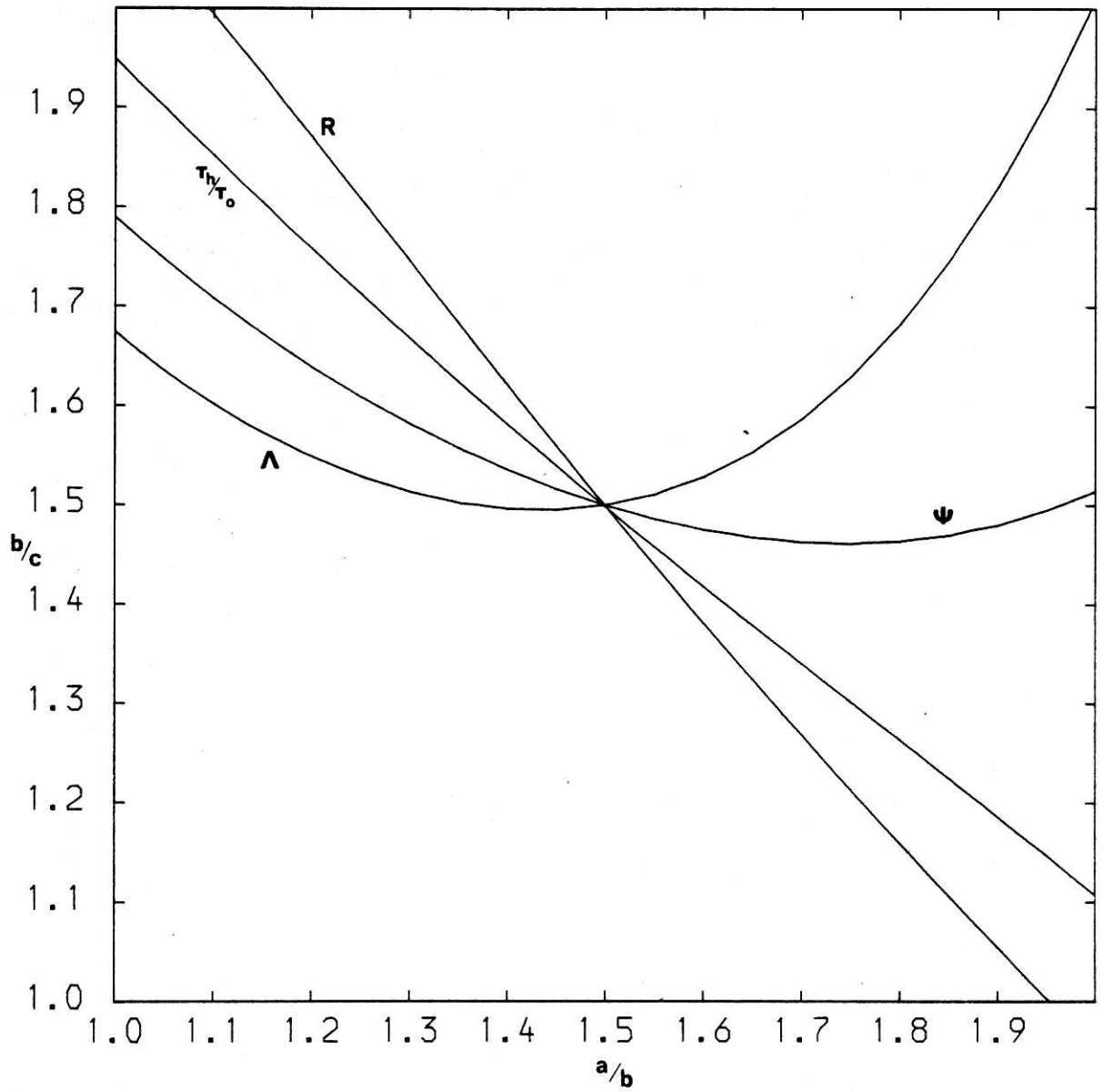


Figure 34. Plots of constant R , Ψ and Λ in the a/b , b/c plane corresponding to $a/b = 1.5$, $b/c = 1.5$

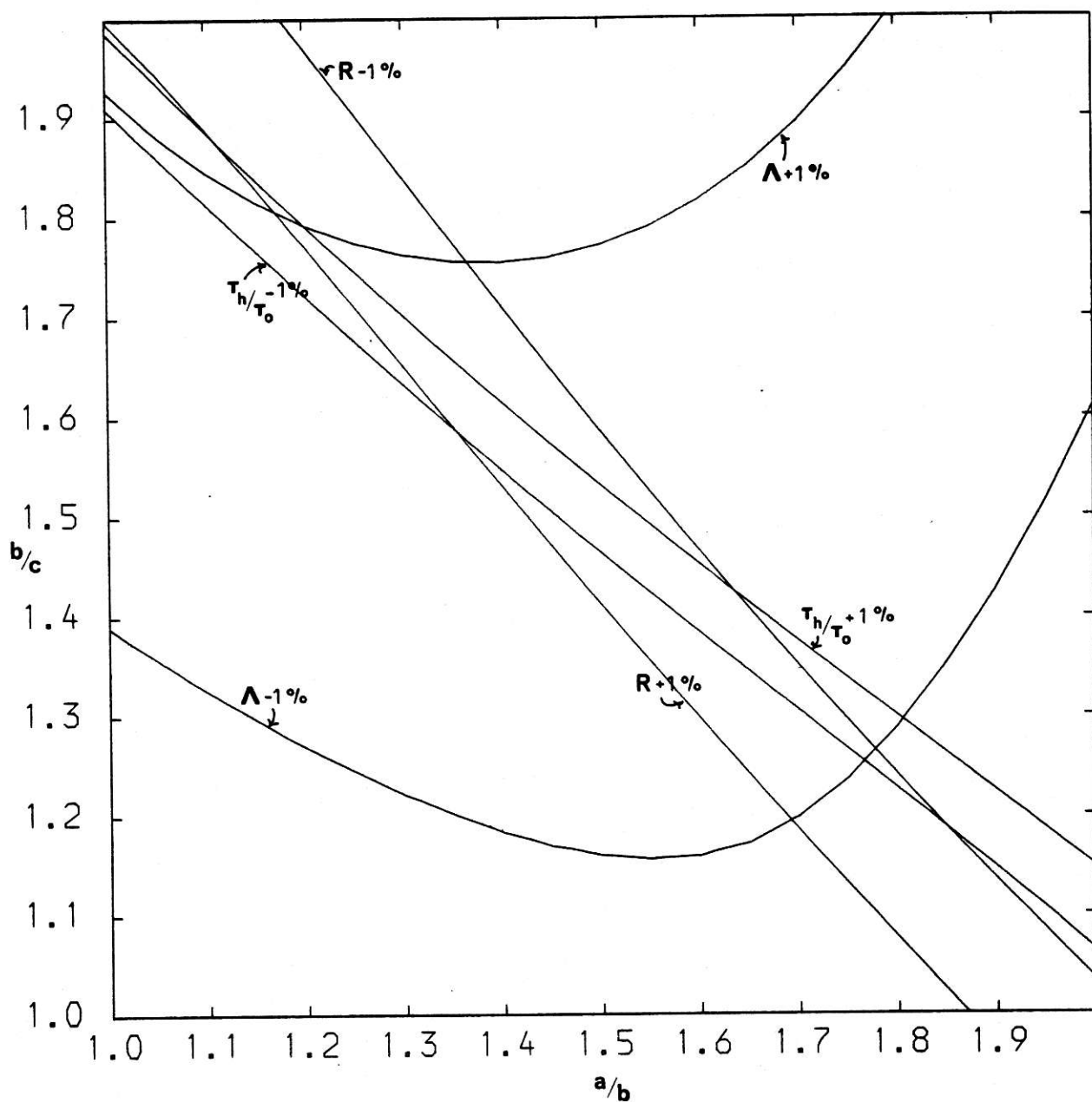


Figure 35. Plots of constant R , Ψ and Λ , allowing for $\pm 1\%$ error in their measured values, in the a/b , b/c plane corresponding to $a/b = 1.5$, $b/c = 1.5$

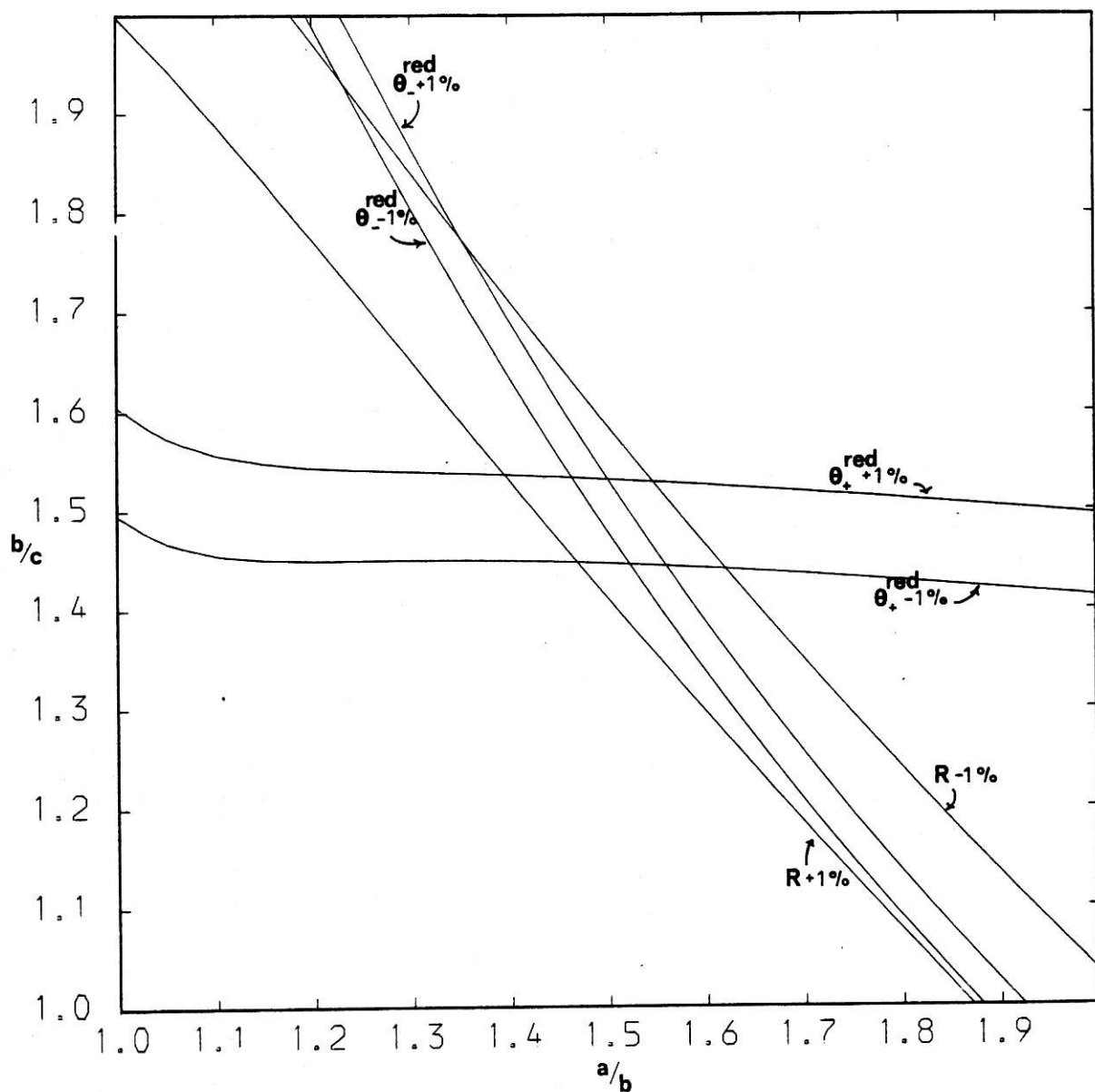


Figure 36. Plots of constant R , θ_+^{red} and θ_-^{red} , allowing for $\pm 1\%$ error in their measured values, in the a/b , b/c plane corresponding to $a/b = 1.5$, $b/c = 1.5$

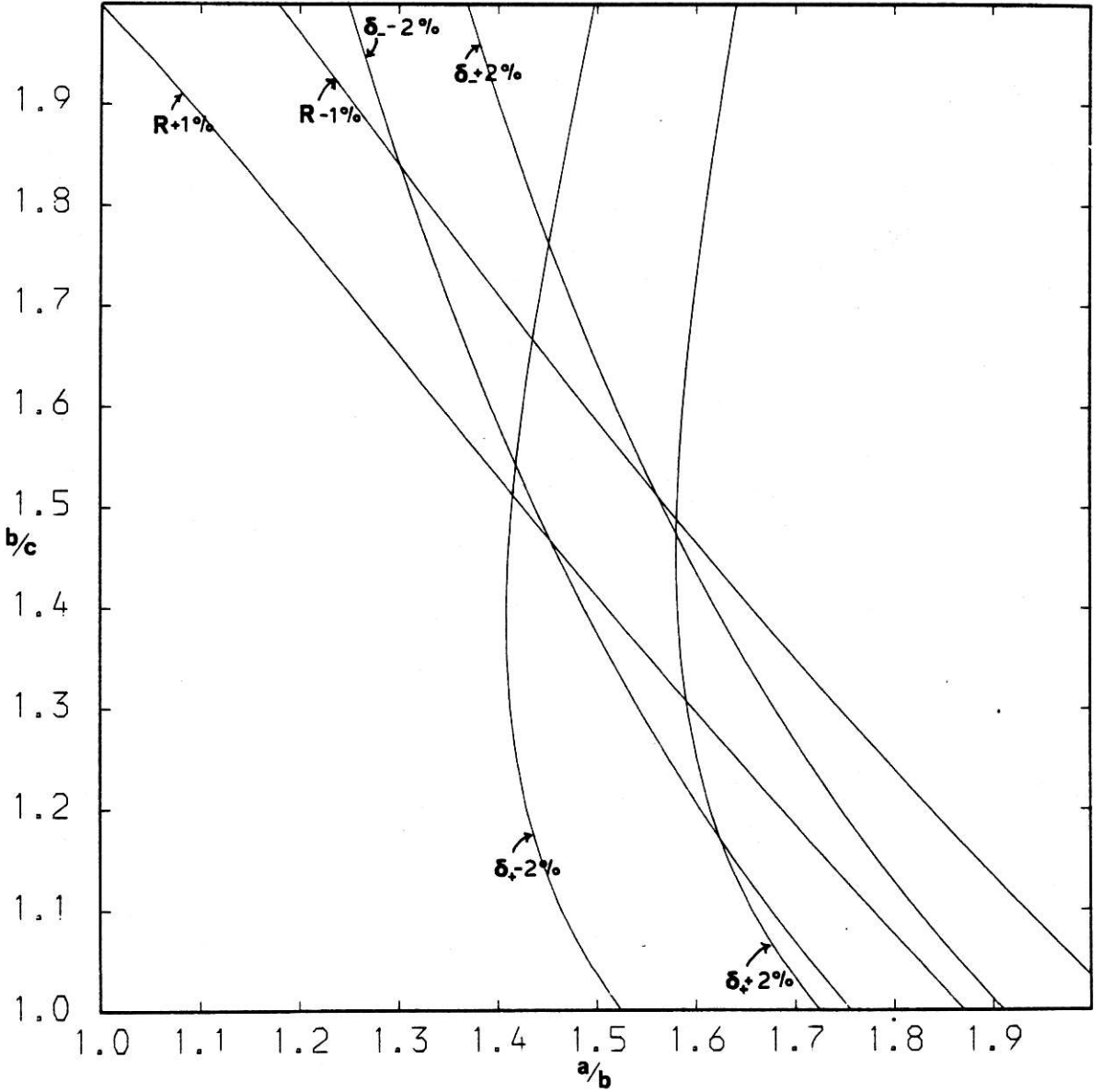


Figure 37. Plots of constant R , δ_+ and δ_- , allowing for $\pm 1\%$ measured error in R and $\pm 2\%$ measured error in δ_{\pm} , in the a/b , b/c plane corresponding to $a/b = 1.5$, $b/c = 1.5$

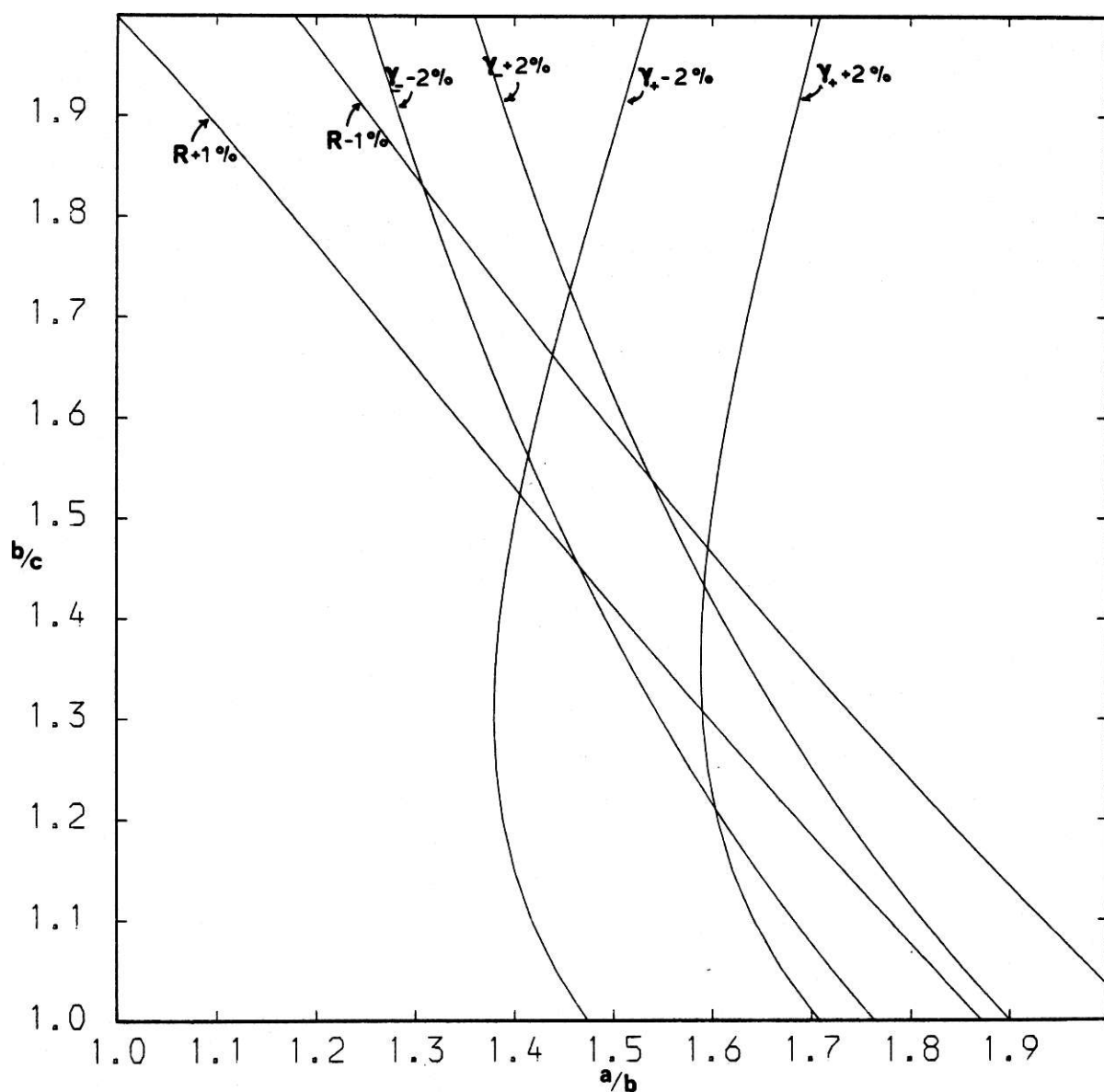


Figure 38. Plots of constant R , γ_+ and γ_- , allowing for $\pm 1\%$ measured error in R and $\pm 2\%$ measured error in γ_{\pm} , in the a/b , b/c plane
corresponding to $a/b = 1.5$, $b/c = 1.5$